Optimal Operation of Contactless Transformers with Resonance in Secondary Circuits

Xun Liu[2], W. M. Ng[1] , C.K. Lee[1] and S. Y. (Ron) Hui[1], *Fellow IEEE*

[1]Center for Power Electronics, City University of Hong Kong
[2]ConvenientPower Ltd., Hong Kong

(email: eeronhui@cityu.edu.hk)

***Abstract* – Contactless transformer is an essential element in inductive power transfer systems. To improve its efficiency performance, a resonant tank is normally formed at the secondary side by adding an external capacitor in series (SS) or in parallel (SP) with the secondary winding. In this paper, a mathematical analysis based on simplified circuit model is presented. It leads to the theory of the boundary frequency which can be used to determine the optimal operating range for *SS* and *SP* mode, respectively, from the efficiency point of view. Calculated and measured results have been given to verify the theory in a case study.**

Keywords- contactless transformer, efficiency, resonance

I. INTRODUCTION

Inductive power transfer without direct physical electrical connection has gained much attention in the past a few years [1, 2]. Inductive electronic chargers have also been proposed [3-5] for contactless applications, which improve the convenience and user-friendliness of portable electronic products, such as mobile phone, MP3, iPod, CD player and etc., because no connectors or cords are needed [6-8].

The general structure of the contactless charging system is shown in Fig.1, in which the contactless transformer is an essential element. The winding connected to an alternating source (transmitter) is called the primary winding. The AC current flowing through the primary winding sets up the alternating magnetic flux and thereby induces an AC voltage in the other winding, called secondary winding. The induced power is then conditioned by the receiver to provide the desired voltage and/or current to the load.

Normally, due to the large leakage inductance or low coupling coefficient in the contactless transformer, a resonant tank is formed at the secondary side by adding an external capacitor, in order to improve its performance [9]. The external capacitor can be connected in parallel [10, 11] or in series [12, 13] with the secondary winding, which are called '*SP*' (Secondary-Parallel) or '*SS*' (Secondary-Series) mode, respectively, in this paper.

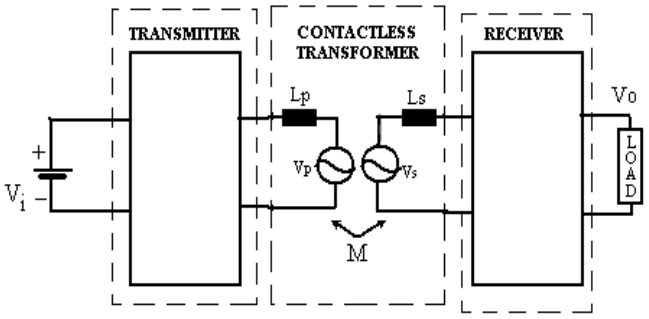

Fig.1. Block diagram of the contactless charging system

In [9] and [14], *SP* and *SS* mode are analyzed and compared from the circuit characteristics point of view. So far, no comparison has been made from the efficiency point of view. In this paper, a boundary frequency is found for optimal operation of contactless transformers under different loading conditions. Such boundary condition is then applied to efficiency analysis in a case study. Finally, some measured results are given to verify the theory.

II. MATHEMATICAL ANALYSIS BASED ON SIMPLIFIED CIRCUIT MODEL

The equivalent circuit of contactless transformer is shown in Fig.2(a). L_p and L_s are used to represent the inductance of primary winding and secondary winding, respectively. The capacitor added at the secondary side is C_s in Fig.2(a), which can be placed in series or in parallel with the secondary winding. R_L is the equivalent resistor of the load.

978-1-4244-1874-9/08/$25.00 ©2008 IEEE

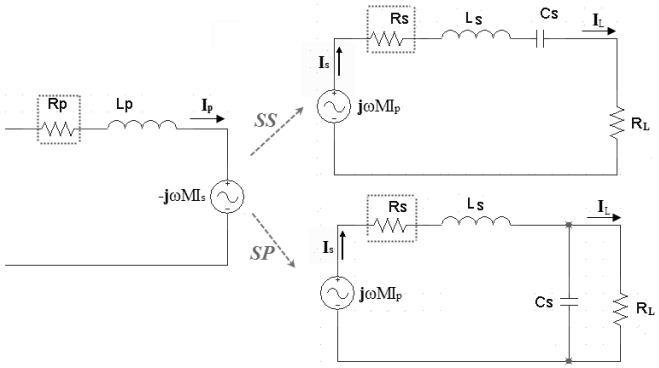

(a) coupled model

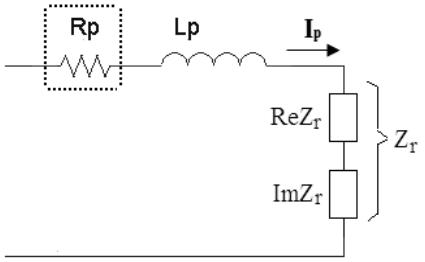

(b) primary side with reflected impedance

Fig.2 The equivalent circuit model of contactless transformer

As a simplified circuit model, the equivalent resistance values of the coupling windings, R_P and R_S, are initially ignored in the first analysis below, because they are normally much smaller than the load resistor, R_L. Their influence will be discussed in the latter part. Fig.2(b) is the equivalent circuit of the primary side with reflected impedance from the secondary circuit, Z_r. The expression of Z_r is given by (1) [9]:

$$Z_r = \frac{\omega^2 M^2}{Z_S} \qquad (1)$$

where Z_S is the lumped impedance of the secondary side and is expressed in (2) for SS and SP, respectively, when R_P and R_S are ignored:

$$Z_S = \begin{cases} j\omega L_S + \dfrac{1}{j\omega C_S} + R_L & \text{(SS)} \\ j\omega L_S + \dfrac{1}{j\omega C_S + \dfrac{1}{R_L}} & \text{(SP)} \end{cases} \qquad (2)$$

Substituting (2) into (1), the reflected resistance and reactance can be derived out:

$$\mathrm{Re}\, Z_r = \begin{cases} \dfrac{\omega^4 C_S^2 M^2 R_L}{(\omega^2 C_S L_S - 1)^2 + \omega^2 C_S^2 R_L^2} & \text{(SS)} \quad (3) \\ \dfrac{\omega^2 M^2 R_L}{R_L^2 (\omega^2 C_S L_S - 1)^2 + \omega^2 L_S^2} & \text{(SP)} \quad (4) \end{cases}$$

and

$$\mathrm{Im}\, Z_r = \begin{cases} \dfrac{-\omega^3 C_S M^2 (\omega^2 C_S L_S - 1)}{(\omega^2 C_S L_S - 1)^2 + \omega^2 C_S^2 R_L^2} & \text{(SS)} \quad (5) \\ \dfrac{-\omega^3 M^2 [C_S R_L^2 (\omega^2 C_S L_S - 1) + L_S]}{R_L^2 (\omega^2 C_S L_S - 1)^2 + \omega^2 L_S^2} & \text{(SP)} \quad (6) \end{cases}$$

If the system works at the resonant frequency of secondary side, that is $\omega = \dfrac{1}{\sqrt{C_S L_S}}$, (3) ~ (6) become the following simple equations:

$$\mathrm{Re}\, Z_r = \begin{cases} \dfrac{\omega^2 M^2}{R_L} & \text{SS} \quad (7) \\ \dfrac{M^2 R_L}{L_S^2} & \text{SP} \quad (8) \end{cases}$$

$$\text{and} \quad \operatorname{Im} Z_r = \begin{cases} 0 & \text{SS} \quad (9) \\ \dfrac{-\omega M^2}{L_S} & \text{SP} \quad (10) \end{cases}$$

By comparing (3), (4) and (7), (8), some conclusions can be drawn for the system working at the resonant frequency of secondary circuit:

For the *SP* mode, $\mathrm{Re}Z_r$ in (8) is the maximum value of $\mathrm{Re}Z_r$ in (4). The maximum reflected resistance exhibited at the resonant frequency is very important to the performance of the contactless transformer. It is under this resonant condition that the maximum efficiency can be achieved. This important point will be demonstrated in this study.

For the *SS* mode, $\mathrm{Re}Z_r$ in (7) may or may not be the maximum value of $\mathrm{Re}Z_r$ in (3). When the frequency increases further ($\omega \to +\infty$), the reflected resistance ($\mathrm{Re}Z_r$) approaches $\dfrac{M^2 R_L}{L_S^2}$ which has the same form as that in (8). Whether $\mathrm{Re}Z_r$ in (7) is the maximum or not depends on the comparison between $\dfrac{\omega^2 M^2}{R_L}$ and $\dfrac{M^2 R_L}{L_S^2}$, or between R_L and ωL_S.

Simple criteria can be derived here as:

(A) If $\omega > \dfrac{R_L}{L_S}$, (ie. $\dfrac{\omega^2 M^2}{R_L} > \dfrac{M^2 R_L}{L_S^2}$), the *SS* mode is better, because $\mathrm{Re}Z_r$ in (7) is the maximum value of $\mathrm{Re}Z_r$ in (3) under this condition.

(B) If $\omega < \dfrac{R_L}{L_S}$, (ie. $\dfrac{\omega^2 M^2}{R_L} < \dfrac{M^2 R_L}{L_S^2}$), the *SP* mode is better, because the maximum reflected resistance can be achieved at a relatively low frequency.

(C) Therefore, $f = \dfrac{R_L}{2\pi L_S}$ is a boundary frequency which can be used for optimal operation of contactless transformer with appropriate resonance at secondary side.

III. Efficiency Analysis

As far as the efficiency is concerned, R_P and R_S must be included, because the ohmic loss of the windings could be the main power loss during operation [15].

Seen from Fig.2(b), no matter the *SS* or *SP* mode is chosen, the input active power dissipates in two parts: R_P and $\mathrm{Re}Z_r$. Then the power absorbed by $\mathrm{Re}Z_r$ can be further divided into two parts: namely, the conduction loss in the secondary winding, R_S, and the load power. The general expression of transformer efficiency η is given by (11):

$$\eta = \eta_P \eta_S \quad (11)$$

where η_p is the efficiency of the primary side and is equal to $\dfrac{\mathrm{Re}\,Z_r}{\mathrm{Re}\,Z_r + R_P}$; η_s represents the efficiency of the secondary side. η_s has different forms for the *SS* and *SP* mode and will be discussed respectively in the following sections.

3.1 The SS Mode

For the SS mode, η_s has a simple expression, that is $\eta_S = \dfrac{R_L}{R_L + R_S}$, because the current flowing through the load, I_L, is the same with the current in the secondary wingding, I_S, as seen from Fig.2(a). If the system always operates at the resonant frequency of secondary side (so that the expression of $\mathrm{Re}Z_r$ is that in (7)), the efficiency of the coupling can be expressed in (12), by substituting η_p, η_s and (7) into (11):

$$Eff(f) = \left(\frac{1}{1 + \dfrac{(R_S(f) + R_L)R_P(f)}{(2\pi f)^2 M^2}} \cdot \frac{R_L}{R_S(f) + R_L} \right) \quad (12)$$

where $R_P(f)$ and $R_S(f)$ represent the winding resistors that are frequency-dependent due to skin effect and proximity effect.

3.2 The SP Mode

The efficiency analysis of *SP* mode is more complicated than the *SS* mode. The efficiency of the secondary side, η_s can be derived as shown in (13).

$$\eta_S = \frac{R_L}{R_L + R_S + R_S R_L^2 \omega^2 C_S^2} \quad (13)$$

By combining (4) and (13) into (11), the calculation of the transformer efficiency can be derived out. Especially, when the secondary side fulfills the resonant condition ($\omega = \frac{1}{\sqrt{C_S L_S}}$) as well as the condition of (B), ReZ_r in (4) reaches its maximum value as expressed by (8), and the efficiency also exhibits a maximum property which is called MEF (Maximum Efficiency Frequency) in [11].

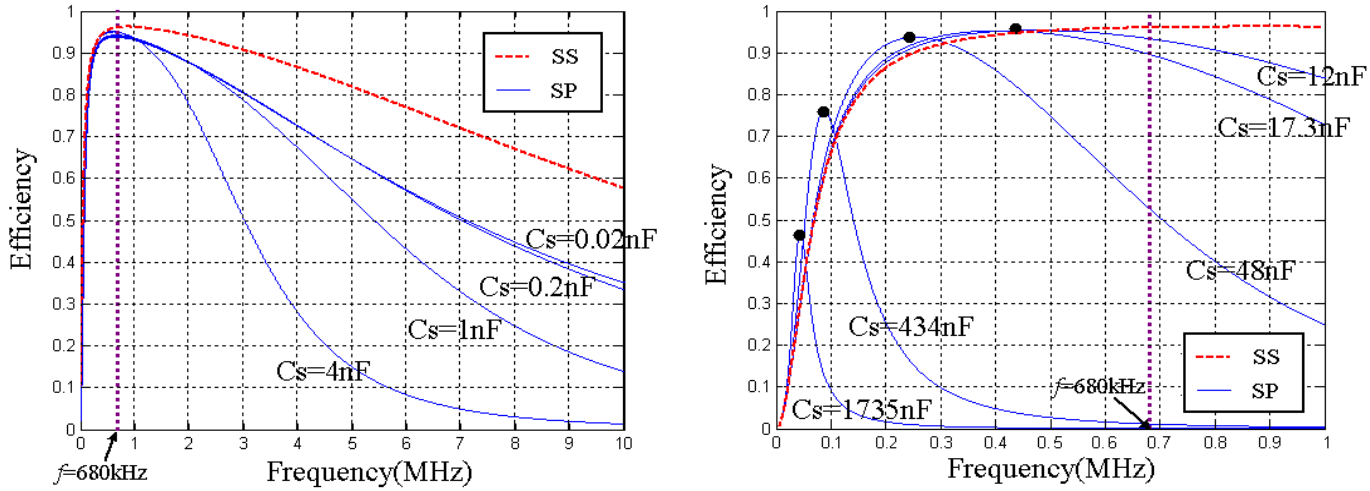

(a) frequency range: **0~10 MHz**

(b) frequency range: **0~1 MHz**

Fig.3. Calculated efficiency when R_L is equal to **25 Ω,** (boundary frequency=**680 kHz**)

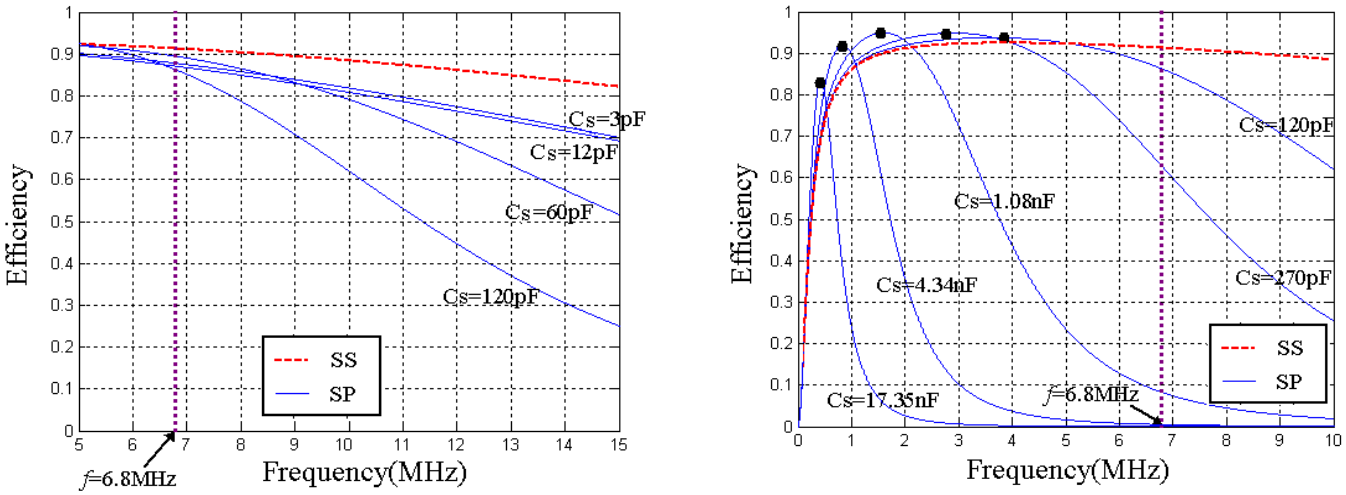

(a) frequency range: **5~15 MHz**

(b) frequency range: **0~10 MHz**

Fig.4 Calculated efficiency when R_L is equal to **250 Ω,** (boundary frequency=**6.8 MHz**)

3.3 A case study

In this case study, two planar spiral windings made by Litz wire are used as the primary and secondary windings, respectively. The inductive parameters of the contactless transformer are given in Table I. The resistance of the windings is frequency-dependant and given by using curve-fitting techniques:

$$R_P = 15\times10^{-14} f^2 + 2.489\times10^{-7} f + 0.1445$$

$$R_S = 15\times10^{-14} f^2 + 2.741\times10^{-7} f + 0.1508$$

where f is the operating frequency in Hertz.

TABLE I. INDUCTIVE PARAMETERS OF THE CONTACTLESS TRANSFORMER

	L_P	L_S	M
Value (μH)	6.067	5.840	4.633

Fig.3 gives the calculated efficiency when the load resistance is 25 Ω. Under this loading condition, the boundary frequency can be estimated as $f_b = \frac{R_L}{2\pi L_S} = 680\text{kHz}$, based on the conclusion of the previous section. The red line is the result of *SS* while tracking the resonant condition of secondary side at different frequencies. Above 680 kHz, *SS* (red line) is always better than *SP* (blue lines), as shown in Fig.3(a). Below the boundary frequency, the maximum efficiency of *SP* is similar to or better than that of *SS,* as shown by the dots in Fig.3(b) . Similar results can be found when the load resistance is increased to 250 Ω, as shown in Fig.4. Under this loading condition, the boundary frequency changes to 6.8 MHz.

IV. MEASURED RESULTS

The measured results are obtained and compared with the calculated results in Fig.5, when R_L equals 25 Ω. Fig.5(a) shows the results when the external capacitor added in the *SP* mode is 1.08 nF. Above the boundary frequency (680 kHz), *SS* is always better than *SP* from the efficiency point of view, no matter what external capacitor is chosen for *SP* (also see Fig.3(a)). However, below the boundary frequency, if an appropriate capacitor is chosen (to make the secondary side resonant below the boundary frequency), the maximum efficiency achieved by *SP* (which is called maximum-efficiency-frequency (MEF) in [11]) can be higher than *SS*, seen from Fig.5(b).

Similar results can also be found in Fig.6, when the load resistance is changed to 250 Ω. Under this loading condition, the boundary frequency changes to 6.8MHz. When an appropriate

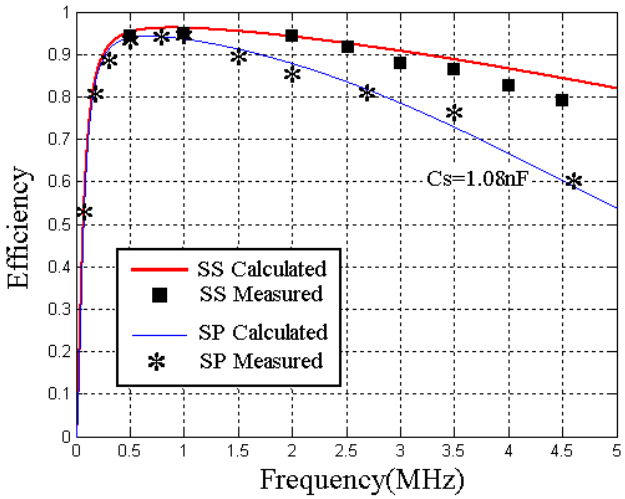

(a) frequency range: **0~5MHz**, $C_{s(SP)}$=1.08 nF

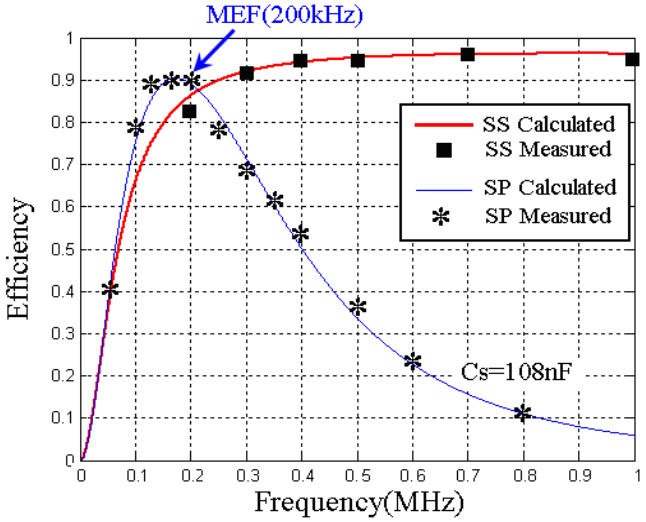

(b) frequency range: **0~1MHz**, $C_{s(SP)}$=108 nF

Fig.5 Measured efficiency when R_L is equal to **25 Ω**

capacitor (C_S=1.08nF) is chosen to be parallel resonant with *Ls* below the boundary frequency (in this case, $f_r = \frac{1}{2\pi\sqrt{C_S L_S}}$=2MHz<6.8MHz), MEF can also be found. It can also be seen from Fig.6 that the actual maximum efficiency exists at a frequency slightly lower than the calculated MEF, because the ac winding resistance increases with operating

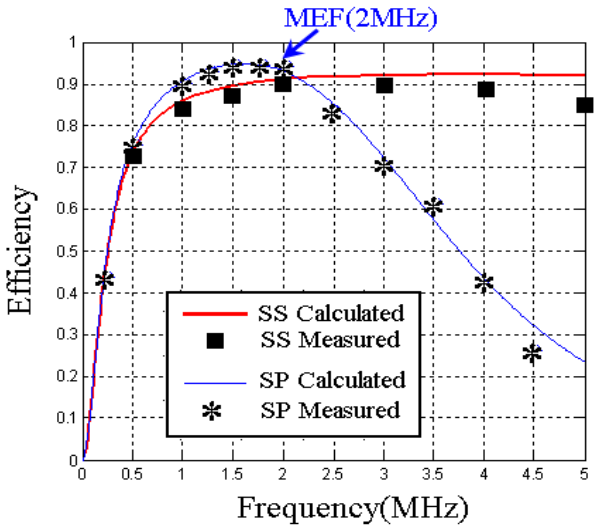

Fig.6 Measured efficiency when R_L is equal to **250 Ω**
Frequency range: 0~5MHz, $C_{s(SP)}$=1.08 nF

frequency. The good agreement between the calculated and measured results also verifies the proposed theory in this paper.

V. CONCLUSIONS

In this paper, a mathematical analysis based on simplified circuit model is presented. It leads to the identification of a boundary frequency which can be used to determine the optimal operating range for *SS* and *SP* mode, respectively, from the efficiency point of view. Calculated and measured results have been given to verify the theory in a case study. The maximum efficiency achieved by *SP* mode only exists within the boundary frequency determined by loading conditions. Outside the boundary frequency, the optimal operation range of contactless transformers is extended by using the *SS* mode [16].

ACKNOWLEDGMENT

The authors are grateful to the Hong Kong Research Grant Council for its support for this project (CityU 114105). The support from the Centre for Power Electronics of the City University of Hong Kong is also acknowledged.

REFERENCES

[1] M. Nishimura, A. Kawamura, G. Kuroda, C. Zhu and E. K. Sato, "High efficient contact-less power transmission system for the high speed trains", in IEEE Power Electronics Specialists Conference, PESC'05, Jun. 2005, pp. 547-553.

[2] T. Bieler, M. Perrottet, V. Nguyen and Y. Perriard, "Contactless power and information transmission", IEEE Transactions on Industrial Applications, vol. 38, no. 5, pp. 1266-1272, Sept.-Oct., 2002.

[3] K. Oguri, "Power supply coupler for battery charger", US Patent 6 356 049, 2000.

[4] Y. Yang and M. Jovanovic, "Contactless electrical energy transmission system", US Patent 6 301 128, 2000.

[5] H. J. Brockmann and H. Turtiainen, "Charger with inductive power transmission for batteries in a mobile electrical device", US Patent 6 118 249, 1999.

[6] B. Choi, J. Nho, H. Cha, T. Ahn and S. Choi, "Design and implementation of low-profile contactless battery charger using planar printed circuit board windings as energy transfer device", IEEE Transactions on Industrial Electronics, vol. 51, no. 1, pp. 140-147, Feb. 2004.

[7] Y. Jang and M. M. Jovanovic, "A contactless electrical energy transmission system for portable-telephone battery chargers", IEEE Transactions on Industrial Electronics, vol. 50, no. 3, pp. 520 – 527, Jun. 2003.

[8] C.-G. Kim, D.-H. Seo, J.-S. You, J.-H. Park and B. H. Cho, "Design of a contactless battery charger for cellular phone", IEEE Transactions on Industrial Electronics, vol. 48, no. 6, pp. 1238-1247, Dec. 2001.

[9] C.-S. Wang, G. A. Covic, and O. H. Stielau, "Power transfer capability and bifurcation phenomena of loosely coupled inductive power transfer systems", IEEE Transactions on Industrial Electronics, vol. 51, no. 1, pp. 148 – 157, Feb. 2004.

[10] H. Abe, H. Sakamoto and K. Harada, "A noncontact charger using resonant converter with parallel capacitor of the secondary coil", IEEE Transactions on Industrial Applications, vol. 36, no. 2, pp. 444-451, Mar. 2000.

[11] S. C. Tang, S. Y. R. Hui and H. Chung, "Coreless planar printed-circuit-board (PCB) transformers—a fundamental concept for signal and energy transfer", IEEE Transactions on Power Electronics, vol. 15. no. 5, pp.931-941, Sept. 2000.

[12] J. Hirai, T.-W. Kim and A. Kawamura, "Study on intelligent battery charging using inductive transmission of power and information", IEEE transactions on Power Electronics, vol. 15, no. 2, pp. 335-345, Mar. 2000.

[13] D. A. G. Pedder, A. D. Brown, and J. A. Skinner, "A contactless electrical energy transmission system," IEEE Transactions on Industrial Electronics, vol. 46, pp. 23–30, Feb. 1999.

[14] C.-S. Wang, O. H. Stielau and G. A. Covic, "Design considerations for a contactless electric vehicle battery charger", IEEE Transactions on Industrial Electronics, vol. 52, no. 5, pp. 1308-1314, Oct. 2005.Y. Jang, and M. M. Jovanovic, "A contactless electrical energy transmission system for portable-telephone battery chargers", *IEEE Transactions on Industrial Electronics*, vol. 50, no. 3, pp. 520 – 527, Jun. 2003.

[15] W. G. Hurley, M. C. Duffy, S. O'Reilly, and S. C. O'Mathuna, "Impedance formulas for planar magnetic structures with spiral windings", IEEE Transactions on Industrial Electronics, vol. 46, no. 2, pp. 271-278, April 1999.

[16] S.Y.R. Hui, "Rechargeable battery circuit and structure for compatibility with a planar inductive charging platform", US patent application US 11/189,097 (filed 25 July 2005) and US 11/234,045 (Filed 23 Sept. 2005)